Laser damage resistance of ion-beam sputtered Sc_2O_3/SiO_2 mixture optical coatings

Mathias Mende[1,*], Stefan Schrameyer[1], Henrik Ehlers[1], Detlev Ristau[1,2], Laurent Gallais[3]

[1]Laser Zentrum Hannover e.V. Hollerithallee 8 D-30419 Hannover, Germany

[2]QUEST: Centre of Quantum Engineering and Space-Time Research, Hannover, Germany

[3]Institut Fresnel, CNRS, Aix-Marseille Université, Ecole Centrale Marseille, Campus de St Jérôme, 13013 Marseille, France

[*]Corresponding author: m.mende@lzh.de

We report on the correlation between the laser damage resistance, the optical and the physical properties of Sc_2O_3/SiO_2 mixture coatings. Several sets of samples with ten different mixture ratios have been prepared by ion-beam sputtering. The atomic compositions of the mixture thin films are quantified employing X-ray photoelectron spectroscopy depth profiles. Laser induced damage thresholds are determined with single sub-picosecond pulses (500fs) at 1030nm. Furthermore, Son1 multi-shot measurements are realized in the ultraviolet wavelength range (355nm) at pulse durations of 5ns. In addition, the influence of two different substrate polishing qualities on the radiation resistance of the composite thin films is discussed.

OCIS codes: 310.0310, 320.0320, 140.3330.

1. Introduction

Dielectric multilayer coatings are an essential part in short pulse laser systems to control the light temporally, spectrally, or spatially. The radiation resistance of these coatings is one of the main limitations in the development of high power lasers especially in the UV wavelength range. In the last years mainly hafnia (HfO_2) as high refractive index material in combination with silica (SiO_2) was in the focus of investigation concerning oxide thin films with highest laser induced damage threshold [1-6]. Another promising high refractive index material is scandia (Sc_2O_3) because of the slightly higher optical band gap (5.7eV) compared to hafnia (5.6eV). In a few studies on the optical and physical properties of single layers [7-9] or for applications in the UV wavelength range [10,11] evaporated scandia coatings have been analyzed. The optical properties and the femtosecond laser damage thresholds of pure scandia single layers deposited by ion beam sputtering are discussed in [12].

The deposition of oxide mixture thin films by ion beam sputtering utilizing a zone target assembly has been demonstrated for various coating material combinations [13,14]. The refractive index and the optical band gap energy of the composite thin films can be adjusted continuously by the atomic composition within the values of co-deposited pure materials. The femtosecond laser damage of those mixture coatings has been investigated for several well-established material combinations at different pulse durations and wavelengths [15,16].

In this study the optical and physical properties of Sc_2O_3/SiO_2 mixture thin films are correlated to the laser induced damage thresholds measured at nano- and femtosecond pulse durations. Furthermore, the influence of two different substrate polishing qualities on the radiation resistance of the mixture coatings is analyzed. The results are interpreted in the context of former investigations on the power handling capability of material mixture coatings.

2. Experimental

2.1 Sample fabrication

The Sc_2O_3/SiO_2 mixture coatings and all the thin films used for the comparison to other composite materials were fabricated in an ion beam sputtering process applying a zone target assembly. The mixing of the sputtered atoms on the atomic level is controlled by the zone target position in the ion beam. The employed Veeco 16cm RF ion source is operated with argon 5.0 purity sputter gas. A more detailed description of the coating plant and some aspects of the deposition process are published in [17]. The two oxide target materials Sc_2O_3 and SiO_2 are specified with a purity of at least 99.99%. The process pressure of the reactive and the sputter gas was $6.9x10^{-5}$mbar for all Sc_2O_3/SiO_2 mixture coatings. Employing a broad band optical monitoring system, a film thickness of two QWOT (quarter-wave optical thickness) at 1,064nm wavelength is precisely realized [18]. The thin films are deposited on silicon wafers and fused silica substrates of two different polishing qualities. Substrate1 is specified with a surface flatness better than lambda/2@633nm and a surface quality of S/D 60/40. Substrate2 is specified with a surface flatness better than lambda/10@633nm, a surface quality of S/D 10/5 and a surface roughness of less than one angstrom RMS. All substrates were pretreated by an automated ultrasonic cleaning system.

2.2 Optical properties

The refractive indices and the extinction coefficients for the Sc_2O_3/SiO_2 mixture series are determined from transmittance and reflectance measurements performed with a Perkin Elmer Lambda 900 and a LZH DUV/VUV spectrophotometer [19]. Figure 1 shows the refractive indices as function of wavelength calculated for Sc_2O_3/SiO_2 mixture thin films with different

compositions (see section 2.3) applying the design software SPEKTRUM [20]. For the determination of the optical band gap energies two different approaches are selected. Both are based on the absorption coefficient α which is calculated from the extinction coefficient. The first method defines the optical band gap E_{04} as the photon energy where the absorption coefficient equals the value of $10^4 cm^{-1}$ [21]. In the second procedure named Tauc Plot, the optical band gap energy E_{Tauc} is determined by plotting $(\alpha h\nu)^{1/2}$ as function of the photon energy hν and extrapolating the linear curve progression to zero [22,23]. In figure 2 the absorption coefficients as function of the photon energy including the E_{04} level (fig. 2a) and the Tauc Plots (fig. 2b) are shown for the different Sc_2O_3/SiO_2 mixture coatings.

2.3 Chemical and structural properties

The chemical composition and the degree of amorphization for the mixture thin films are analyzed by X-Ray Photoelectron Spectroscopy (XPS) and X-Ray Diffraction (XRD). The XPS depth profile measurements are performed with a PHI Quantera SXM instrument employing monochromatic Al Kα X-rays (1486.6eV). The X-ray beam had a diameter of 100μm, and the photoelectron take-off angle was 45° measured from the sample surface plane. The sputter gun was operated with argon gas at an acceleration voltage of 3kV to remove the thin film on a surface area of one square millimeter. During the depth profile measurement the signal of the Sc2p, the Si2p, and the O1s peaks is recorded for film thickness steps of 15nm which correspond to the XPS information depth of 5 to 10nm. In figure 3 high-resolution XPS spectra of the Sc2p (fig. 3a), the Si2p (fig. 3b), and the O1s (fig. 3c) peaks determined for the Sc_2O_3/SiO_2 mixture thin film [(3)] are shown. The O1s signal exhibits two components which are associated with the oxygen bound to scandium and silicon respectively. In figure 4 the calculated atomic concentrations of the three elements Sc, Si, and O are plotted as a function of the sputter depth

for the same Sc_2O_3/SiO_2 mixture thin film. Since the standard deviation of the measured concentrations is smaller than 0.5% for the ten mixture coatings it is reasonable to define mean values for the composition. For the correlation of the composition with the optical properties and the damage thresholds, the Sc fraction of the sum of the Sc and the Si content in the thin film is used as parameter. In figure 5 the Sc fraction with the unit A% (atom %) is shown as a function of the zone target position (black squares). Taking into account that a scandia molecule is composed of two Sc and three O atoms whereas a silica molecule consists of one Si and two O atoms a molecular composition can be calculated from the measured Sc and Si contents of each mixture coating. The Sc_2O_3 fraction of the sum of the Sc_2O_3 and the SiO_2 content with the unit M% (molecule %) is also plotted as a function of the zone target position in figure 5 (red triangles). Furthermore, the measured oxidation ratio (green crosses) is compared to the theoretical ratio calculated on the basis of the molecular compositions (blue dots). A result obtained from the XPS measurements is that the mixture thin films with the higher Sc fractions show greater oxidation ratios than expected from the molecular compositions. This result is in accordance with the stoichiometric ratios (O/Sc) of 1.73 to 1.76 published in [12] for pure scandia thin films.

The micro structure of the mixture coatings is investigated by XRD employing Cu Kα radiation (0.154nm) at a grazing angle of 0.6°. The measurements are performed using a PANalytical X‘Pert PRO MRD instrument. In the diffraction patterns no sharp peaks indicating a crystalline structure as described in [9] are observed. The spectra of four thin films with different compositions are presented exemplarily in figure 6. The broad peak at 22° corresponds to the SiO_2 content in the thin film and to the fused silica substrate [14]. The peak at 32° is attributed to

the Sc_2O_3 content in the coating. In conclusion, the XRD analysis reveals, that all Sc_2O_3/SiO_2 mixture thin films are amorphous.

2.4 Laser induced damage threshold measurements

For this study two laser damage test facilities operating at different pulse durations and wavelengths are applied to analyze the irradiation resistance of the Sc_2O_3/SiO_2 mixture thin films.

The laser damage test set-up and the calibration procedures used for the sub-picosecond tests at 1030nm are described in detail in [24]. The laser source is a commercial femtosecond diode-pumped ytterbium amplified laser (Amplitudes Systemes S-Pulse HP) with a Gaussian spatial beam profile. The operating wavelength is 1030nm with a 5nm spectral bandwidth. The pulse duration is 510+/-10fs, measured with a single-shot autocorrelator. The laser beam is linearly polarized, at normal incidence on the sample, and focused on the front face of the coated sample by a planoconvex lens (focal length 150mm). A beam diameter of 49µm at 1/e is measured at the location of the sample using the effective spot size as defined in the corresponding ISO standard [25]. Considering the uncertainties in the energy and beam profile measurements, the error on the fluence determination is estimated to be 4% for the tests made in this study. The samples have been tested using the 1on1 mode (one irradiation by site) with 30 sites tested for each fluence value. The damage detection was done with a Zeiss Axiotech microscope under a X100 objective. Damage was defined as any modification observed in the irradiated area with Nomarski or dark field mode.

For the nanosecond tests at 355nm a diode-pumped Nd:YAG laser (InnoLas Spitlight DPSS 250) with a Gaussian spatial beam profile is employed. After third harmonic generation a pulse duration of 5ns (FWHM) is measured with a photodiode. The linear polarized laser beam is

focused on the coating surface at normal incidence. The effective beam diameter is set to approximately 200µm at the target plane. Each coating is tested on more than 150 sites in 10,000on1 mode applying a repetition rate of 100Hz. The occurrence of laser induced damage during the pulse series is detected online by monitoring the scattered light with a photodiode. Again damage was defined as any modification observed in the irradiated area by Nomarski microscopy. The measurement and evaluation procedure is performed according to the ISO standard [25] using ten different classes of pulse numbers to generate the characteristic damage curve. For the comparison of the measurement results the 0% threshold value of the 10,000 pulse class is applied. The error budget of the fluence determination is estimated to be 25% considering the uncertainties in the stability of the laser system and the beam profile as well as the beam energy measurements.

3. Results and discussion

3.1 Laser induced damage thresholds and morphologies

The sub-picosecond laser damage thresholds measured at 1030nm wavelength are plotted as a function of the Sc fraction of the sum of the Sc and the Si content in figure 7a. The results are presented in terms of "internal" LIDT and "measured" LIDT, using (1)

$$\mathrm{LIDT}_{\mathrm{internal}} = \left|\mathrm{E}_{\mathrm{max}} / \mathrm{E}_{\mathrm{inc}}\right|^2 \mathrm{LIDT}_{\mathrm{measured}} \quad (1)$$

with E_{max} / E_{inc} being the ratio of the maximum of the standing-wave electric field distribution in the film to the incident electric field. This ratio is calculated numerically based on the determined refractive index and film thickness. Several conclusions can be drawn when analyzing these results.

The first remark is that there is no distinguishable difference in the LIDT between samples deposited on the substrates with the different polishing qualities. This result is in contrast to results in the nanosecond regime where the cleaning and polishing process have a significant influence on the coating LIDT at 1064nm wavelength [26].

Secondly, the evolution of the measured LIDT as function of the thin film composition shows a complex behavior. Starting from pure silica and increasing the scandium fraction, a small decay of the LIDT for the first four samples, then an increase of the LIDT for fractions higher than 50% up to 75% scandium and finally a decrease of the LIDT for fractions above 75% scandium is observed. This behavior is different from other mixture materials that have been tested before [16]. Looking at the optical band gap energies of the samples that evolve monotonically with the thin film composition (see figure 12) it is obvious that the complex behavior of the LIDT is induced by another thin film property and not by the optical band gap energy. It has been shown for instance that by co-deposition of coating materials the crystalline micro structure of high index thin films can be disrupted and result in an amorphous structure [27,28]. Since the XRD analysis of the Sc_2O_3/SiO_2 mixture thin films has shown amorphous micro structures, the physical explanation for the optimum of the LIDT is unclear. An analysis of the laser damage morphologies has been done by scanning electron (SEM) and Nomarski (NM) microscopy for a deeper understanding. The sub-picosecond laser damage morphologies for Sc_2O_3/SiO_2 mixture coatings with different compositions are presented in Figure 8. Typical images observed at fluences approximately 25% higher than the LIDT are shown. The morphologies can be divided in two classes and linked to the measured LIDT in the following way:

- For the samples with a scandium fraction between 0 and 65% the damage morphologies are very similar and it is not possible to see differences between the samples with our instruments. This is consistent with a weak evolution of the LIDT from sample to sample.
- For scandium fractions above 75% melting effects can be observed and an evolution of the damage morphologies is evidenced. At the center of the irradiated area the film has been removed but on the edges a melted area is visible. The size of the melted area is decreasing for increasing scandium fractions

The damage morphology transition between these two regimes is marked by the dashed line in figure 7a. From these results it is obvious that to understand the dependence of the damage threshold from the mixture composition, thermal effects need to be taken into account.

The measured nanosecond laser damage thresholds at 355nm are plotted as a function of the Sc fraction of the sum of the Sc and the Si content in figure 9. A significant discrepancy in the measured 0% threshold value of the 10,000 pulse class is observed between the coatings on the two types of substrates with different polishing qualities. Starting from the pure scandia thin film, where no deviation is measured, the influence of the polishing quality raises continuously with the decreasing scandium fraction. For the pure silica coating the difference of the laser damage threshold is approximately 100%, which is much more than the difference of the uncoated substrates. To understand this discrepancy the damage morphologies for both substrate types have been analyzed by Nomarski microscopy. The damage morphologies presented in figure 10 show a defect induced damage behavior as expected for this pulse duration and wavelength. Starting from pure scandia and increasing the silicon fraction a transition from rather large lateral damage in the range of the beam diameter to a damage consisting of small separated pits is observed. A similar development of the damage morphologies has been found

for HfO_2/SiO_2 mixture thin films deposited on substrate1 [6]. Comparing the damage morphologies for the two different polishing qualities, substrate1 shows significantly more separated pits than substrate2. These pits can be interpreted as damage caused by defects of the substrate surface influencing the interface with the coating. From these results it is obvious that the damage thresholds measured for mixture coatings with high silicon fractions are affected by the polishing quality. This needs to be taken into account to understand the dependence of the damage threshold from the mixture composition in the nanosecond regime.

3.2 Correlation between optical properties, chemical composition and laser damage threshold

The relation between the refractive indices and the chemical compositions of mixture thin films prepared by different deposition techniques is investigated in several studies using effective medium approximation theories [14,29,30]. The refractive indices of oxide mixture coatings can be calculated from the refractive indices and the molar volume fractions of the co-deposited pure materials applying the Lorentz-Lorenz model [31,32]. In equation (2) n_{eff} represents the refractive index of mixture thin film, whereas n_a and n_b are the refractive indices of the used pure materials, respectively.

$$\frac{n_{eff}^2 - 1}{n_{eff}^2 + 2} = f_a \frac{n_a^2 - 1}{n_a^2 + 2} + f_b \frac{n_b^2 - 1}{n_b^2 + 2} \quad (2)$$

The two filling factors $f_{a/b}$ are determined from the molar volume fractions $v_{a/b}$ via (3).

$$f_{a/b} = \frac{v_{a/b}}{v_a + v_b} = \frac{\frac{S_{a/b} M_{a/b}}{\rho_{a/b}}}{\frac{S_a M_a}{\rho_a} + \frac{S_b M_b}{\rho_b}} \quad (3)$$

For the molecular fractions $S_{a/b}$ the results of the XPS depth profile measurements are inserted. The mass densities $\rho_{a/b}$ of the co-sputtered pure materials are assumed to be comparable to the bulk values of 3.86g/cm^3 for Sc_2O_3 and 2.20g/cm^3 for SiO_2. The molar masses $M_{a/b}$ are 137.91g/mol for Sc_2O_3 and 60.08g/mol for SiO_2, respectively. In figure 11 the refractive indices derived from transmittance and reflectance measurements and the calculated refractive indices are plotted as function of the Sc fraction of the sum of the Sc and the Si content for the two wavelengths 355nm and 1030nm. The two curves show an acceptable agreement for both wavelengths, although a small deviation in the curvature is observed. This discrepancy can be explained by the slightly different mass density of IBS fabricated mixture thin films compared to bulk material values. In conclusion, the relation between the obtained refractive indices and the measured chemical compositions is in accordance with the Lorentz-Lorenz model.

The influence of the chemical composition on the shift of the optical band gap energy has been studied for different ion beam sputtered composite thin films [33,34,6]. For the material combinations TiO_2/SiO_2, Ta_2O_5/SiO_2, and HfO_2/SiO_2 a non-linear increase of the optical band gap energy above a silica volume fraction of 75% is reported. The composition dependence of the optical band gap energies derived by the E_{04} and the Tauc approach is illustrated in figure 12. For the Sc_2O_3/SiO_2 mixture thin films an almost linear behavior with a slight non-linear increase towards high silica volume fractions is observed. The results from both approaches show a similar curve progression with an offset of approximately 0.2eV for the E_{04} values. For the correlation of the optical band gap energy with the femtosecond damage thresholds the results derived by the Tauc Plot approach are applied.

The laser damage threshold for femtosecond pulse durations is reported to be determined by the intrinsic coating material properties rather than by defects and impurities of the dielectric film.

The relation between the internal single-pulse damage fluence F_{th} and the optical band gap energy E_g can be described via equation (4) [35].

$$F_{th} \approx (c_1 E_g + c_2)\, \tau_p^{\kappa} \quad (4)$$

Where τ_p represents the pulse duration and c_1, c_2, and κ are material independent constants. In figure 7b the damage fluences calculated via equation (4) using the constants including error estimations published in [35] (blue solid line and gray dashed line) are compared to the internal damage fluences derived from the measurements (red squares). Because of the significant discrepancy between the calculated and the measured internal damage fluences, a second linear fit is introduced to achieve an acceptable accordance for the Sc_2O_3/SiO_2 mixture thin films (green dash-dot line). For a more precise description of the measured damage fluences an extensive model taking into account thermal effects [36] has to be applied, but this will go beyond the scope of this paper.

3.3 Comparison to other optical materials

In figure 13 the femtosecond damage thresholds of the Sc_2O_3/SiO_2 mixture thin films are compared to 1on1 results for other pure and mixture material coatings deposited on substrate1. The internal damage threshold of 3.1J/cm^2 for the pure scandia film appears quite high. For other high index material thin films, tested under the same conditions and deposited in the same coating plant, internal damage thresholds of 2.5J/cm² (Al_2O_3), 1.7J/cm² (HfO_2) and 1.1J/cm² (Ta_2O_5) are obtained [16]. Based on this result, a Sc_2O_3(60%)/SiO_2(40%) mixture as high index material combined with silica as low index material looks like a promising combination for the fabrication of optical interference coatings used in high power applications. However, the multi-pulse LIDT has not been measured in this study, therefore the results should be taken with

caution for practical applications since the femtosecond LIDT of dielectric coatings for multi-pulse exposure is lower compared to single-pulse illumination [35].

A comparison between the nanosecond damage threshold of the Sc_2O_3/SiO_2 mixture thin films and results for other pure and mixture material coatings deposited on substrate1 is not discussed because of the evidenced influence of the inferior substrate polishing quality.

4. Conclusions

The deposition of amorphous Sc_2O_3/SiO_2 mixture thin films has been realized by ion beam sputtering applying a zone target set-up. The atomic compositions of the mixture thin films quantified by X-ray photoelectron spectroscopy depth profile measurements show a homogeneous distribution as a function of the film thickness. For mixture thin films with higher Sc fractions slightly higher oxidation ratios than expected from the calculated molecular compositions are measured. The refractive indices derived from spectral measurements are in good agreement with the values calculated via the Lorentz-Lorenz model from the atomic compositions. An almost linear shift of the optical band gap energy as a function of the thin film composition has been found applying two different evaluation approaches. For the sub-picosecond damage thresholds analyzed in dependence of the optical band gap energy deviations from the law and the error estimations published by Mero et. al. are observed. Compared to the results measured for mixture coatings consisting of other high refractive index materials in combination with silica, relatively high damage thresholds have been measured for the Sc_2O_3/SiO_2 thin films with larger scandium fractions. From these results Sc_2O_3/SiO_2 mixtures seem to be a promising choice to produce optical interference coatings for high power applications in the femtosecond pulse duration range. In contrast to the sub-picosecond LIDT at

1030nm, where no difference between the two types of fused silica substrate is observed, a significant influence of the polishing quality is found for the nanosecond LIDT at 355nm. The deviation of the LIDT values for the two substrate types raises continuously from 0% for the pure scandia thin film to approximately 100% for the pure silica coating. This effect will be in the focus of further investigations and needs to be taken into account to understand the dependence of the damage threshold at 355nm from the mixture composition in the nanosecond pulse regime.

5. Acknowledgements

The authors thank the German Federal Ministry of Economics and Technology (BMWi) for the financial support of the research project “TAILOR” under contract no. 16IN0667 within the framework of the “InnoNet” program. Also, funding by the German Research Foundation (DFG) within the Cluster of Excellence 201, “Centre of Quantum Engineering and Space Time Research”, QUEST, is gratefully acknowledged. Furthermore the authors are grateful to Mr. Bernd Bock from the Tascon GmbH for performing the XPS-measurements and to Dr. Jan Petersen from the Fraunhofer IST for making the XRD-measurement. Finally the support from the "Réseau des Technologies Femtosecondes" (CNRS/MRCT) is appreciated for the determination of the sub-picosecond laser damage thresholds.

6. References

1. S. M. J. Akhtar, D. Ristau, J. Ebert, and H. Welling, "Characterization of Dielectric Films and Damage Threshold at 1.064µm", Phys. Stat. Sol. (a) **115**, 191 (1989)
2. B. Andre, L. Poupinet, and G. Ravel, "Evaporation and ion assisted deposition of HfO_2 coatings: Some key points for high power applications", J. Vac. Sci. Technol. A **18**, 2372 (2000)
3. C. J. Stolz, M. D. Thomas and A. J. Griffin, "BDS thin film damage competition", Proc. SPIE **7132**, 71320C (2008)
4. B. Langdon, D. Patel, E. Krous, J. J. Rocca, C.S. Menoni, F. Tomasel, S. Kholi, P. R. McCurdy, P. Langston, and A. Ogloza, "Influence of process conditions on the optical properties HfO_2/SiO_2 thin films for high power laser coatings", Proc. SPIE **6720**, 67200X (2007)
5. L. Gallais, B. Mangote, M. Zerrad, M. Commandré, A. Melninkaitis, J. Mirauskas, M. Jeskevic, and V. Sirutkaitis, "Laser-induced damage of hafnia coatings as a function of pulse duration in the femtosecond to nanosecond range", Appl. Opt. **50**, 178–187 (2011)
6. L. O. Jensen, M. Mende, H. Blaschke, D. Ristau, D. Nguyen, L. Emmert, and W. Rudolph, „Investigations on SiO_2/HfO_2 mixtures for nanosecond and femtosecond pulses",Proc. SPIE **7842**, 784207 (2010)
7. W. Heitmann, "Reactively Evaporated Films of Scandia and Yttria" Appl. Opt. **12**, 394–397 (1973)
8. M. F. Al-Kuhaili, "Optical properties of scandium oxide films prepared by electron beam evaporation", Thin Solid Films **426,** 178–185 (2003)

9. G. Liu, Y. Jin, H. He, and Z. Fan, “Effect of substrate temperatures on the optical properties of evaporated Sc_2O_3 thin films”, Thin Solid Films **518**, 2920–2923 (2010)
10. F. Rainer, W. H. Lowdermilk, D. Milam, T. Tuttle Hart, T. L. Lichtenstein, and C. K. Carniglia, ”Scandium oxide coatings for high-power UV laser applications”, Appl. Opt. **21**, 3685–3688 (1982)
11. S. Tamura, S. Kimura, Y. Sato, H. Yoshida, and K. Yoshida, “Laser-damage threshold of Sc_2O_3/SiO_2 high reflector coatings for a laser wavelength of 355nm”, Thin Solid Films **228**, 222–224 (1993)
12. C. S. Menoni, E. M. Krous, D. Patel, P. Langston, J. Tollerud, D. N. Nguyen, L. A. Emmert, A. Markosyan, R. Route, M. Fejer, and W. Rudolph, "Advances in ion beam sputtered Sc_2O_3 for optical interference coatings", Proc. SPIE **7842**, 784202 (2010)
13. M. Lappschies, B. Görtz, and D. Ristau, “Application of optical broadband monitoring to quasi-rugate filters by ion-beam sputtering”, Appl. Opt. **45**, 1502–1506 (2006)
14. A. Melninkaitis, T. Tolenis, L. Mažulė, J. Mirauskas, V. Sirutkaitis, B. Mangote, X. Fu, M. Zerrad, L. Gallais, M. Commandré, S. Kičas, and R. Drazdys, “Characterization of zirconia–and niobia–silica mixture coatings produced by ion-beam sputtering”, Appl. Opt. **50**, C188–C196 (2011)
15. D. Nguyen, L. A. Emmert, I. V. Cravetchi, M. Mero, W. Rudolph, M. Jupe, M. Lappschies, K. Starke, and D. Ristau, “$Ti_xSi_{1-x}O_2$ optical coatings with tunable index and their response to intense subpicosecond laser pulse irradiation”, Appl. Phys. Lett. **93**, 261903 (2008)
16. B. Mangote, L. Gallais, M. Commandré, M. Mende, L. Jensen, H. Ehlers, M. Jupé, D. Ristau, A. Melninkaitis, J. Mirauskas, V. Sirutkaitis, S. Kičas, T. Tolenis, and R. Drazdys,

"Femtosecond laser damage resistance of oxide and mixture oxide optical coatings", Opt. Lett. **37**, 1478–1480 (2012)

17. M. Mende, L. O. Jensen, H. Ehlers, W. Riggers, H. Blaschke and D. Ristau, "Laser-induced damage of pure and mixture material high reflectors for 355nm and 1064nm wavelength", Proc. SPIE **8168**, 816821 (2011)
18. D. Ristau, H. Ehlers, T. Gross, and M. Lappschies, "Optical broadband monitoring of conventional and ion processes", Appl. Opt. **45**, 1495–1501 (2006)
19. H. Blaschke, J. Kohlhaas, P. Kadkhoda, and D. Ristau, "DUV/VUV spectrophotometry for high precision spectral characterization", Proc. SPIE **4932**, 536 (2003)
20. M. Dieckmann, "SPEKTRUM, Thin Film Design Software", Laser Zentrum Hannover e.V., 1990–2012
21. E. C. Freeman, and William Paul, "Optical constants of rf sputtered hydrogenated amorphous Si", Phys. Rev. B **20**, 716–728 (1979)
22. J. Tauc, R. Grigorovici, and A. Vancu, "Optical properties and electronic structure of amorphous germanium", Phys. Status Solidi B **15**, 627–637 (1966)
23. G. D. Cody, T. Tiedje, B. Abeles, B. Brooks, and Y. Goldstein, "Disorder and the optical-absorption edge of hydrogenated amorphous silicon", Phys. Rev. Lett. **47**, 1480–1483 (1981)
24. B. Mangote, L. Gallais, M. Zerrad, F. Lemarchand, L. H. Gao, M. Commandré, and M. Lequime, "A high accuracy femto-/picosecond laser damage test facility dedicated to the study of optical thin films", Rev. Sci. Instrum. **83**, 013109 (2012)
25. ISO 21254:2011, "Test methods for laser-induced damage threshold", International Organization for Standardization

26. H. Krol, L. Gallais, M. Commandré, C. Grézes-Besset, D. Torricini, and G. Lagier, "Influence of polishing and cleaning on the laser-induced damage threshold of substrates and coatings at 1064nm," Opt. Eng. **46**, 023402 (2007)
27. B. J. Pond, J. I. DeBar, C. K. Carniglia, and T. Raj, "Stress reduction in ion beam sputtered mixed oxide films", Appl. Opt. **28**, 2800–2805 (1989)
28. C.-C. Lee and C.-J. Tang, "TiO_2-Ta_2O_5 composite thin films deposited by radio frequency ion-beam sputtering", Appl. Opt. **45**, 9125–9131 (2006)
29. X. Wang, H. Masumoto, Y. Someno, and T. Hirai, "Microstructure and optical properties of amorphous TiO_2 - SiO_2 composite films synthesized by helicon plasma sputtering", Thin Solid Films **338**, 105–109 (1999)
30. J.-S. Chen, S. Chao, J.-S. Kao, H. Niu, and C.-H. Chen, "Mixed films of TiO_2 - SiO_2 deposited by double electron-beam coevaporation", Appl. Opt. **35**, 90–96 (1996)
31. H. A. Lorentz, "Über die Beziehung zwischen der Fortpflanzungsgeschwindigkeit des Lichtes und der Körperdichte", Annalen der Physik und Chemie **245**, 641–665 (1880)
32. L. Lorenz, "Über die Refractionsconstante", Annalen der Physik und Chemie **247**, 70–103 (1880)
33. H. Demiryont, "Optical properties of SiO_2 - TiO_2 composite films", Appl. Opt. **24**, 2547–2650 (1985)
34. M. Cevro, "Ion-beam sputtering of $(Ta_2O_5)_x$ - $(SiO_2)_{1-x}$ composite thin films", Thin Solid Films **258,** 91–103 (1995)
35. M. Mero, B. Clapp, J. C. Jasapara, W. Rudolph, D. Ristau, K. Starke, J. Krüger, S. Martin, and W. Kautek, "On the damage behavior of dielectric films when illuminated with multiple femtosecond laser pulses", Opt. Eng. **44**, 051107 (2005)

36. M. Jupé, M. Mende, C. Kolleck, D. Ristau, L. Gallais, and B. Mangote, “Measurement and calculation of ternary oxide mixtures for thin films for ultra short pulse laser optics”, Proc. SPIE **8190**, 819004 (2011)

List of figure and table captions:

1. Fig. 1 (Color online) Refractive index as function of wavelength from 300nm to 1200nm for different Sc_2O_3/SiO_2 mixture thin films.
2. Fig. 2 (Color online) Absorption coefficient as function of photon energy (fig. 2a), and Tauc plots (fig. 2b) for Sc_2O_3/SiO_2 mixture coatings with different compositions.
3. Fig. 3 (Color online) High-resolution XPS spectra of Sc2p (fig. 3a), Si2p (fig. 3b), and O1s (fig. 3c) peaks measured at a Sc_2O_3/SiO_2 mixture thin film (86.1% Sc fraction of the Sc+Si content).
4. Fig. 4 (Color online) XPS depth profile of a Sc_2O_3/SiO_2 mixture coating (86.1% Sc fraction of the Sc+Si content).
5. Fig. 5 (Color online) Measured atomic and calculated molecular composition as function of the zone target position (left axis), and comparison between the theoretical and the measured oxidation ratio (right axis).
6. Fig. 6 (Color online) XRD spectra of amorphous Sc_2O_3/SiO_2 mixture thin films with different compositions.
7. Fig. 7 (Color online) Measured and internal 1on1 LIDT@1030nm as function of the Sc fraction of the Sc+Si content for both types of substrates (fig. 7a), and comparison of the internal damage thresholds as function of the optical band gap energy with the results calculated applying equation (4) (fig. 7b).
8. Fig. 8 (Color online) Nomarski (NM) and scanning electron microscopy (SEM) images of damage morphologies created during 1on1 LIDT measurements at 1030nm.
9. Fig. 9 (Color online) 10,000on1 LIDT@355nm as function of the Sc fraction of the Sc+Si content for both types of substrates including LIDT-values for the uncoated substrates.

10. Fig. 10 (Color online) Nomarski microscopy images of damage morphologies created during 10,000on1 LIDT measurements at 355nm performed on two different substrate types (S1: sample1, S2: sample2).
11. Fig. 11 (Color online) Refractive index at 355nm and at 1030nm as function of the Sc fraction of the Sc+Si content derived from spectral measurements and calculated via equation (2) from the measured compositions.
12. Fig. 12 (Color online) Comparison of E_{Tauc} and E_{04} optical band gap energies as function of the Sc fraction of the Sc+Si content.
13. Fig. 13 (Color online) Comparison of 1on1 LIDT@1030nm as function of the refractive index for different sets of mixture thin films consisting of the material combinations Sc_2O_3/SiO_2, Ta_2O_5/SiO_2, HfO_2/SiO_2 and Al_2O_3/SiO_2.

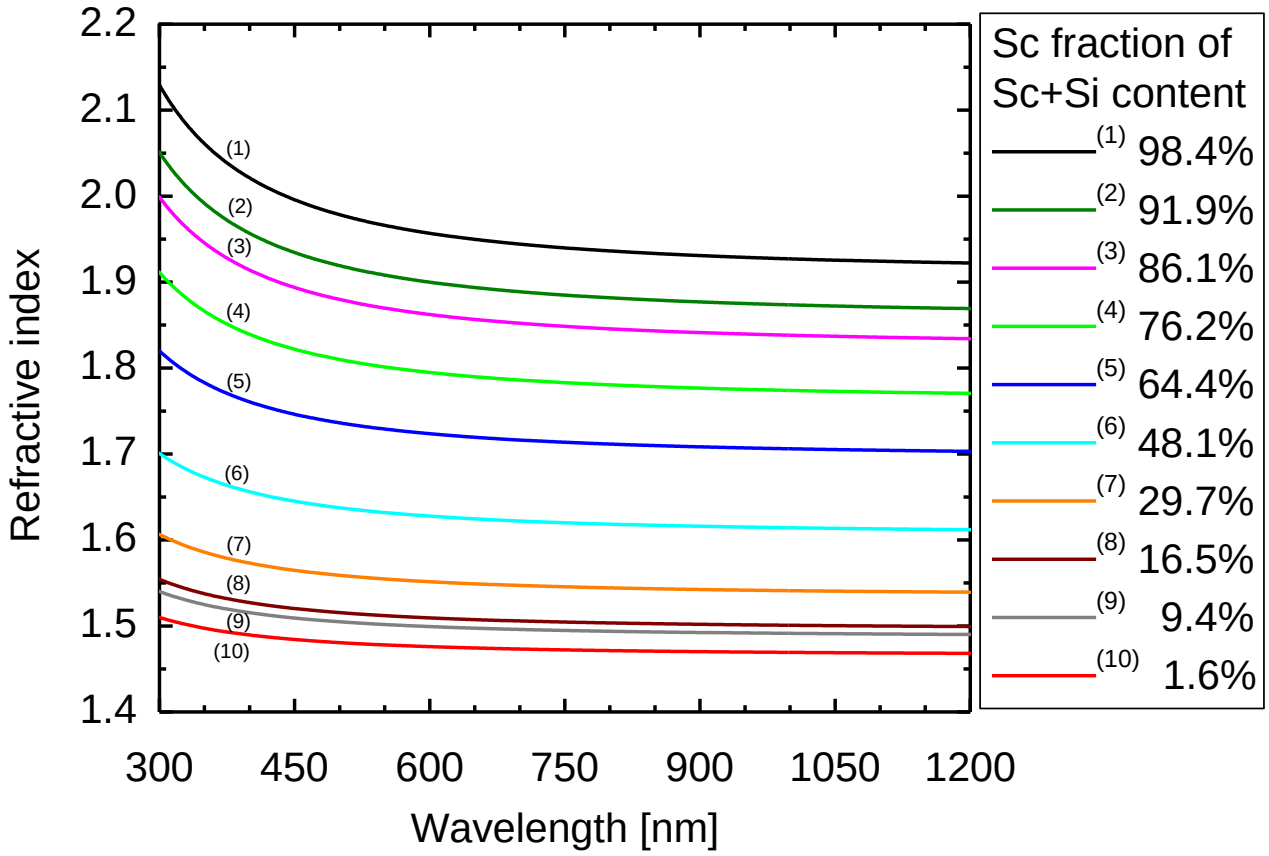
Refractive index
2.2
2.1
2.0
1.9
1.8
1.7
1.6
1.5
1.4
300
450
600
750
900
1050
1200
Wavelength [nm]
(1)
(2)
(3)
(4)
(5)
(6)
(7)
(8)
(9)
(10)
Sc fraction of
Sc+Si content
(1) 98.4%
(2) 91.9%
(3) 86.1%
(4) 76.2%
(5) 64.4%
(6) 48.1%
(7) 29.7%
(8) 16.5%
(9) 9.4%
(10) 1.6%

Fig. 1

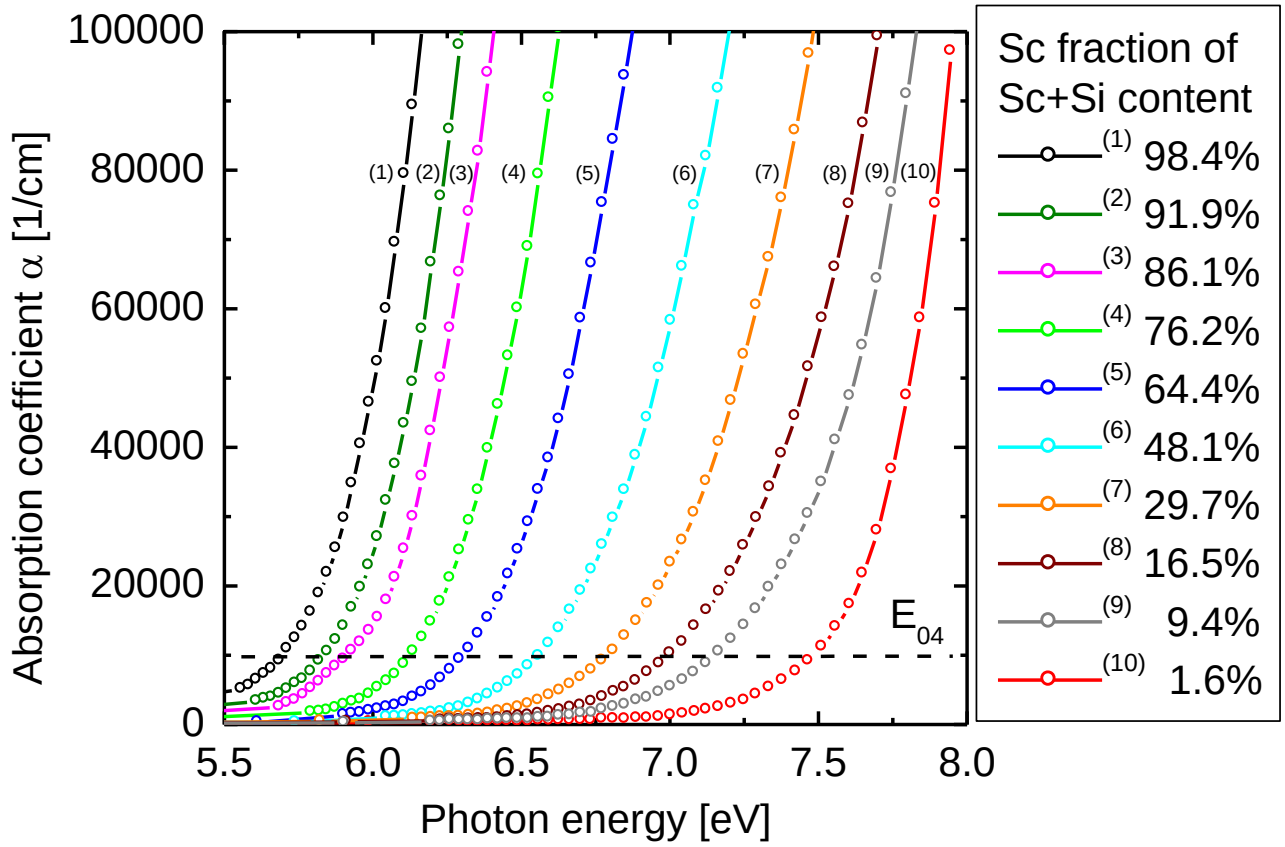
Absorption coefficient α [1/cm]
100000
80000
60000
40000
20000
0
5.5
6.0
6.5
7.0
7.5
8.0
Photon energy [eV]
(1)
(2)
(3)
(4)
(5)
(6)
(7)
(8)
(9)
(10)
E04
Sc fraction of Sc+Si content
(1) 98.4%
(2) 91.9%
(3) 86.1%
(4) 76.2%
(5) 64.4%
(6) 48.1%
(7) 29.7%
(8) 16.5%
(9) 9.4%
(10) 1.6%

Fig. 2a

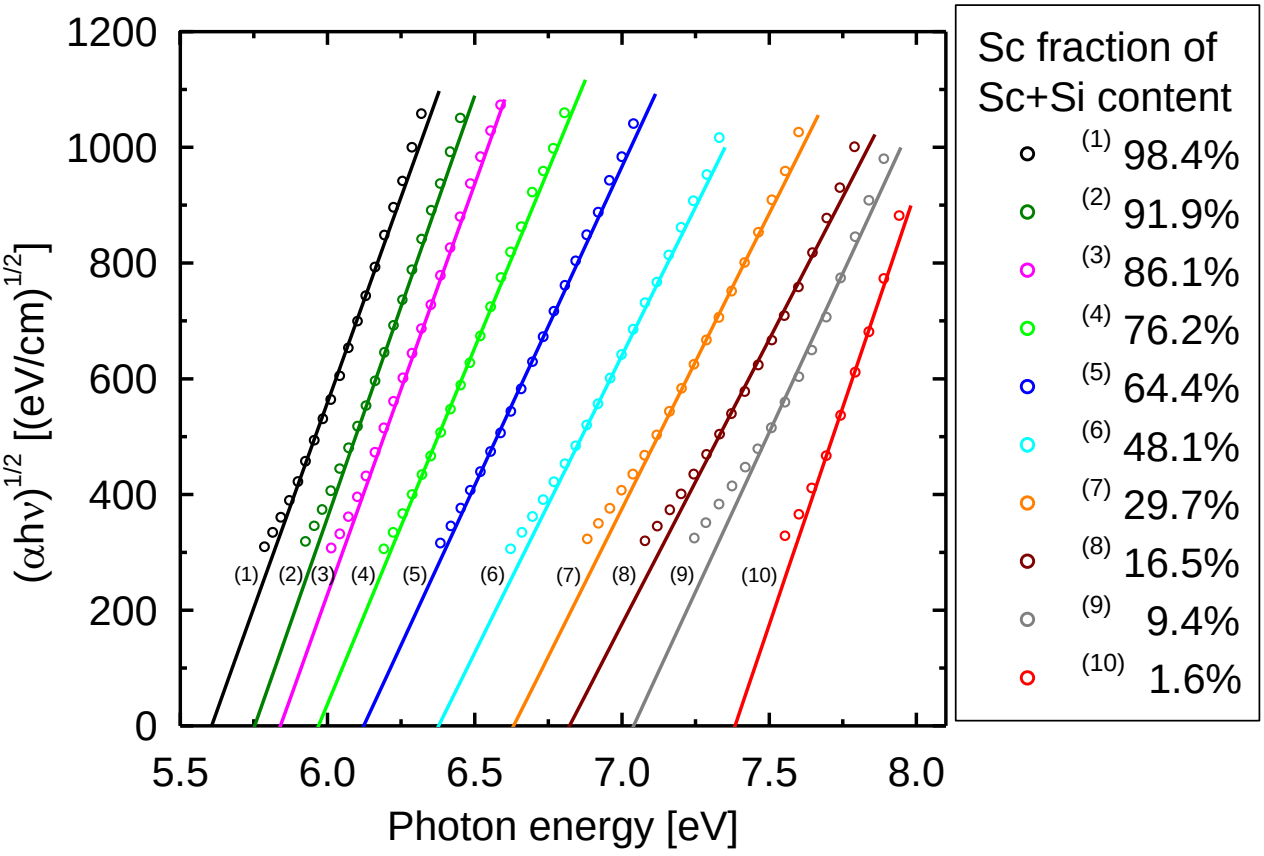
1200
1000
800
600
400
200
0
5.5
6.0
6.5
7.0
7.5
8.0
Photon energy [eV]
(αhν)^1/2 [(eV/cm)^1/2]
(1)
(2)
(3)
(4)
(5)
(6)
(7)
(8)
(9)
(10)
Sc fraction of Sc+Si content
(1) 98.4%
(2) 91.9%
(3) 86.1%
(4) 76.2%
(5) 64.4%
(6) 48.1%
(7) 29.7%
(8) 16.5%
(9) 9.4%
(10) 1.6%

Fig. 2b

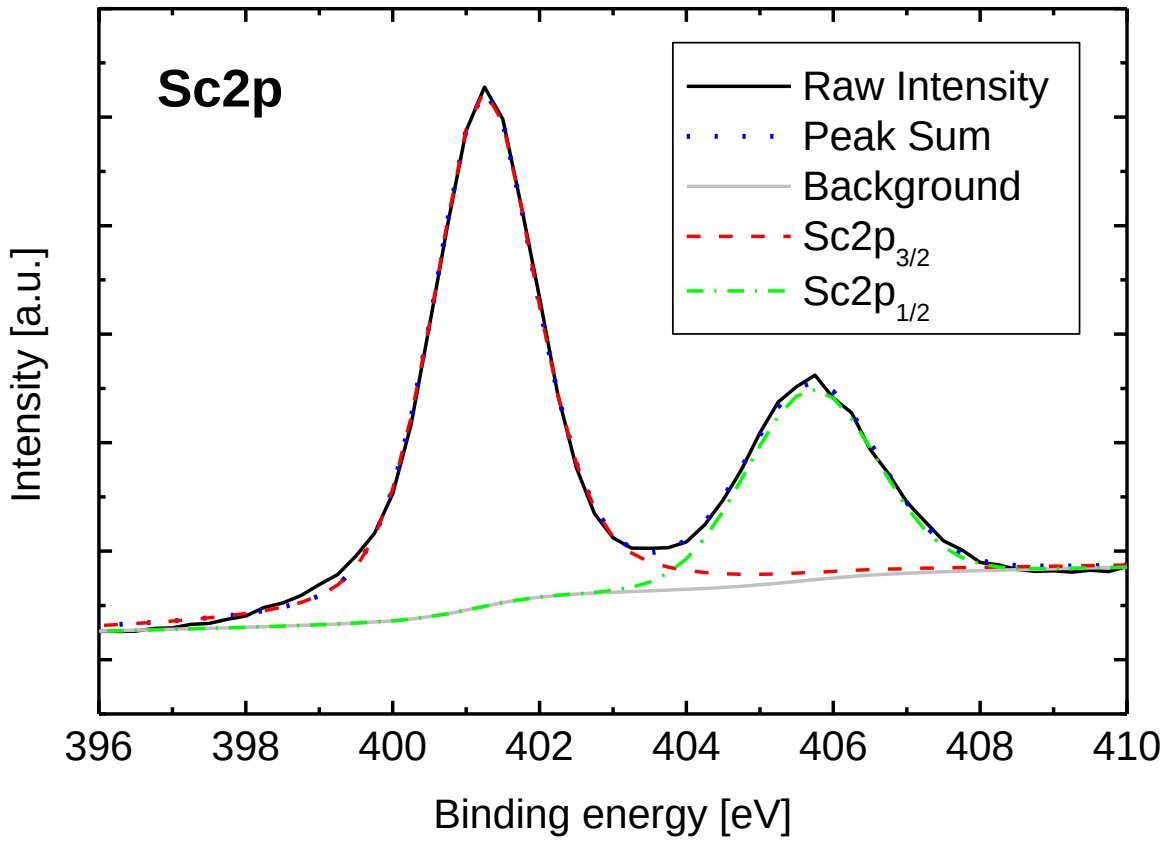
Sc2p
Raw Intensity
Peak Sum
Background
Sc2p3/2
Sc2p1/2
Intensity [a.u.]
396
398
400
402
404
406
408
410
Binding energy [eV]

Fig. 3a

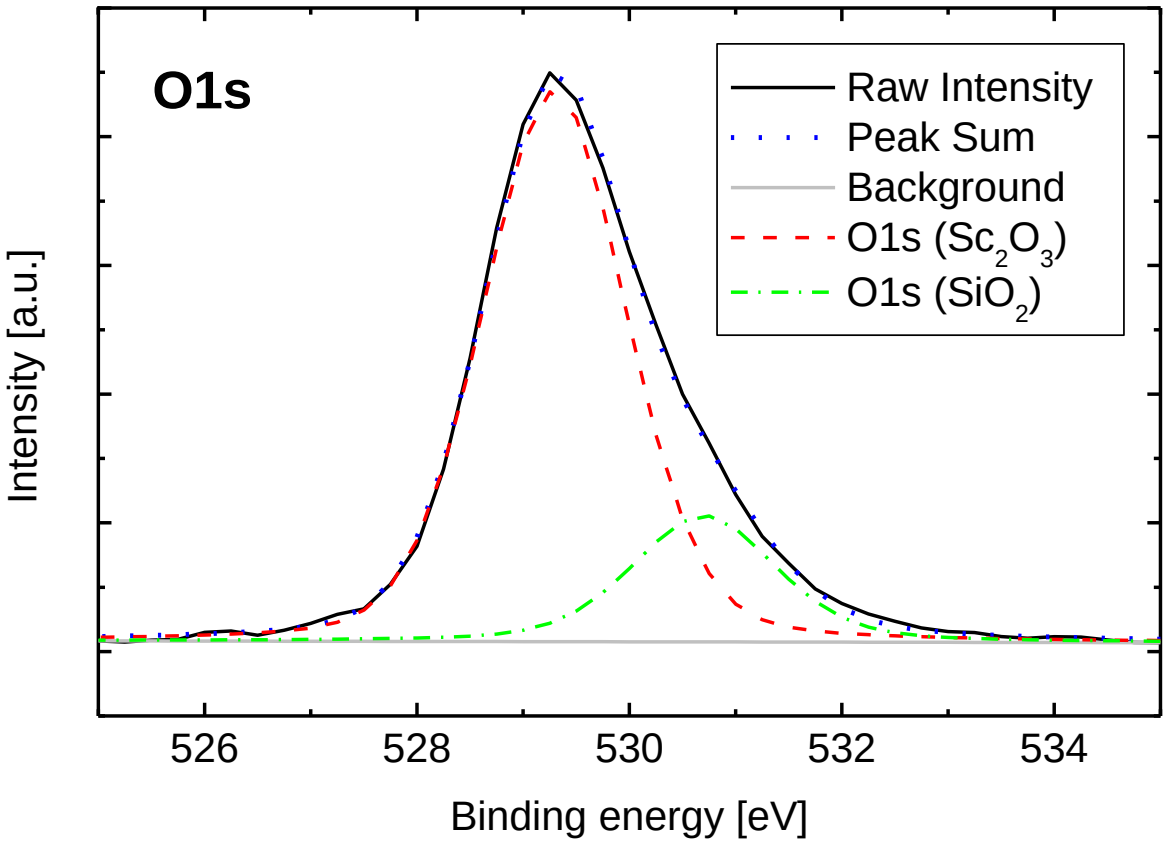
O1s
Raw Intensity
Peak Sum
Background
O1s (Sc2O3)
O1s (SiO2)
Intensity [a.u.]
526
528
530
532
534
Binding energy [eV]

Fig. 3b

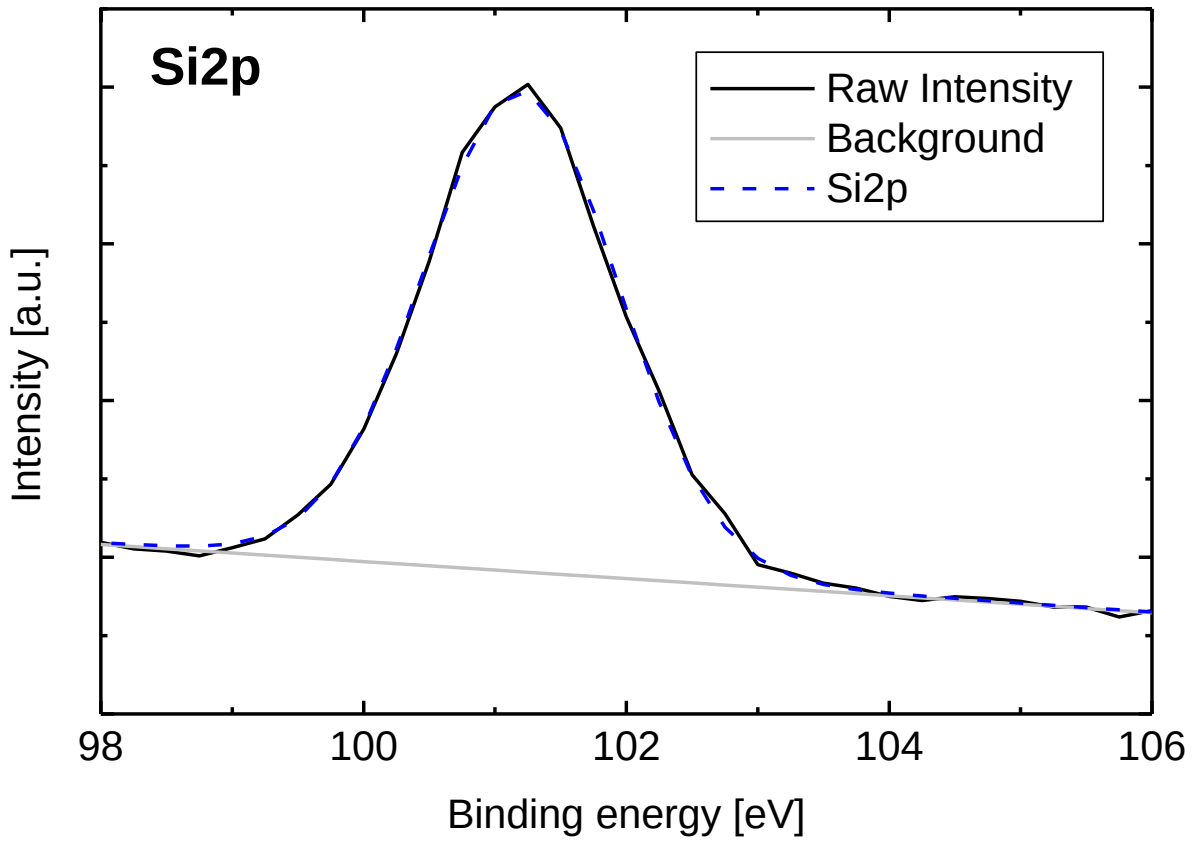
Si2p
Raw Intensity
Background
Si2p
Intensity [a.u.]
98
100
102
104
106
Binding energy [eV]

Fig. 3c

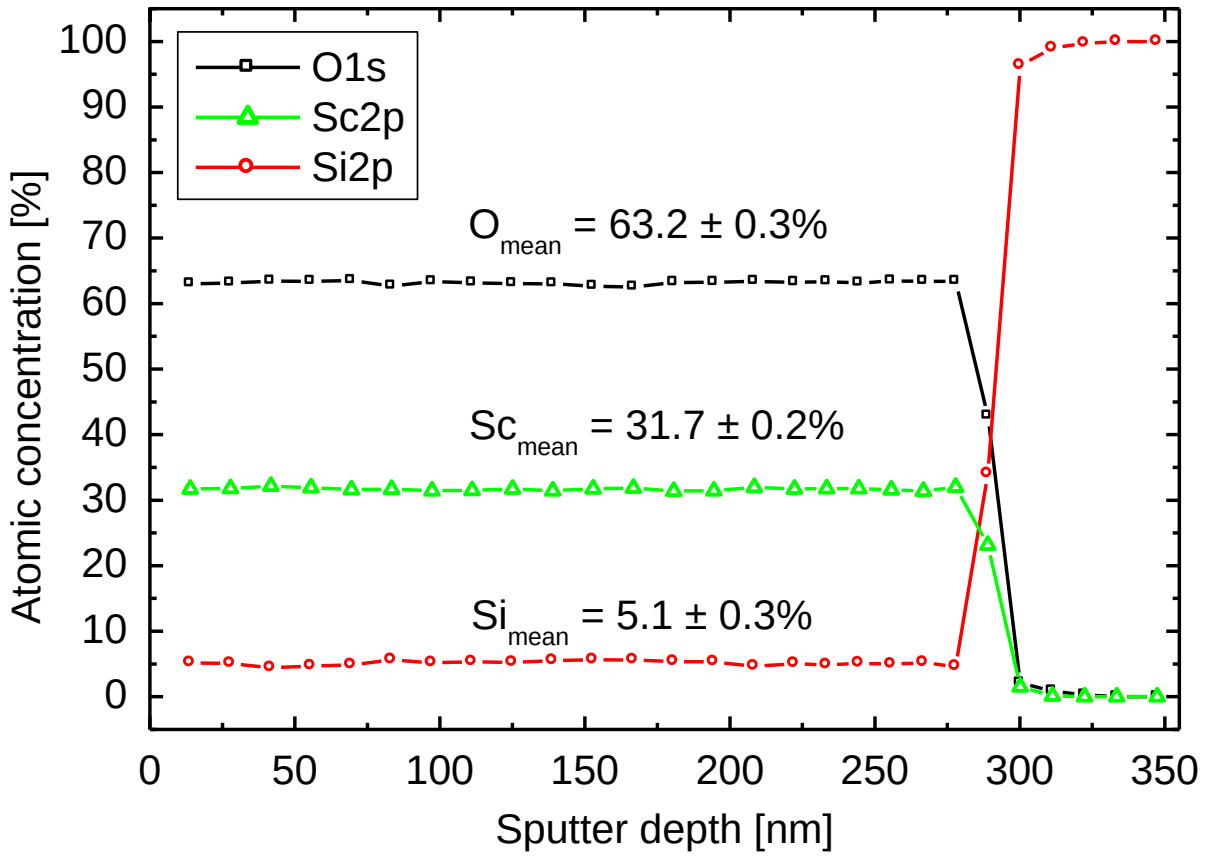
O1s
Sc2p
Si2p
O$_{mean}$ = 63.2 ± 0.3%
Sc$_{mean}$ = 31.7 ± 0.2%
Si$_{mean}$ = 5.1 ± 0.3%
Atomic concentration [%]
Sputter depth [nm]
0
10
20
30
40
50
60
70
80
90
100
0
50
100
150
200
250
300
350

Fig. 4

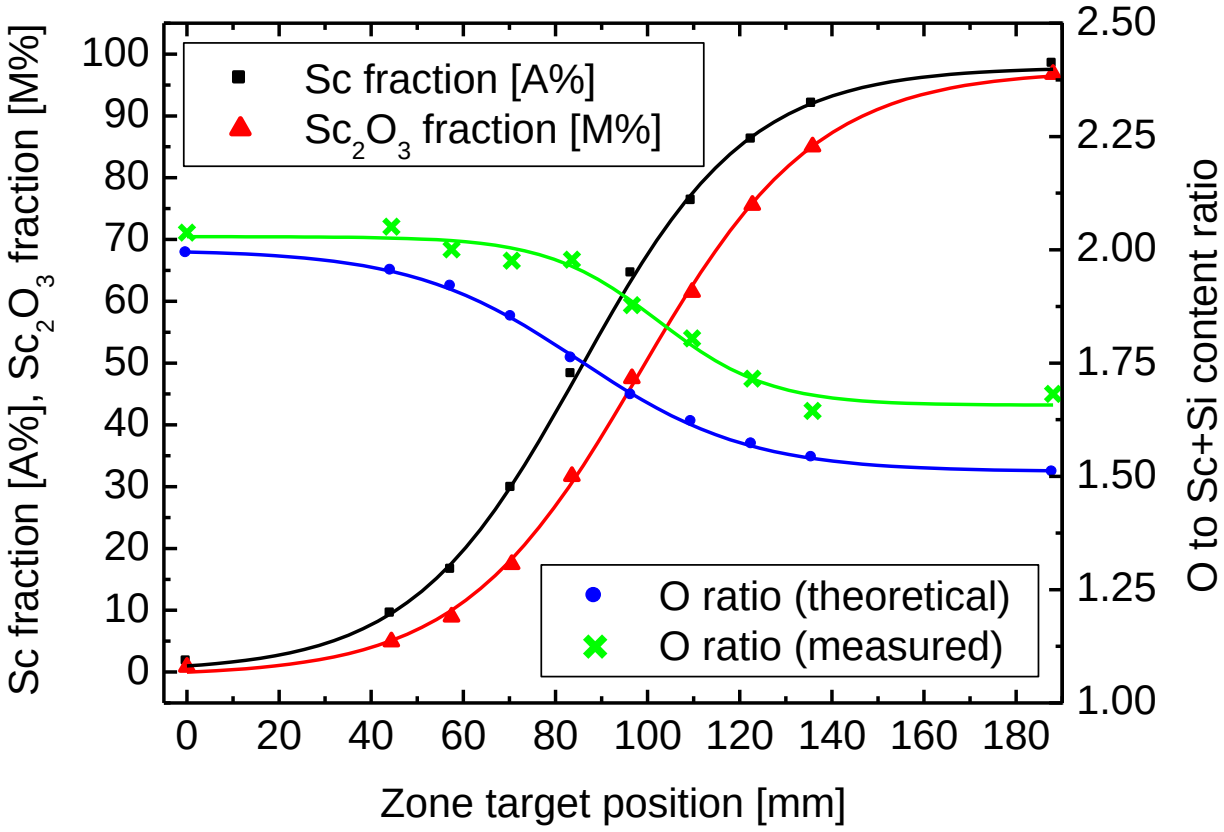
Sc fraction [A%]
Sc2O3 fraction [M%]
O ratio (theoretical)
O ratio (measured)
Sc fraction [A%], Sc2O3 fraction [M%]
O to Sc+Si content ratio
Zone target position [mm]
0
10
20
30
40
50
60
70
80
90
100
0
20
40
60
80
100
120
140
160
180
1.00
1.25
1.50
1.75
2.00
2.25
2.50

Fig. 5

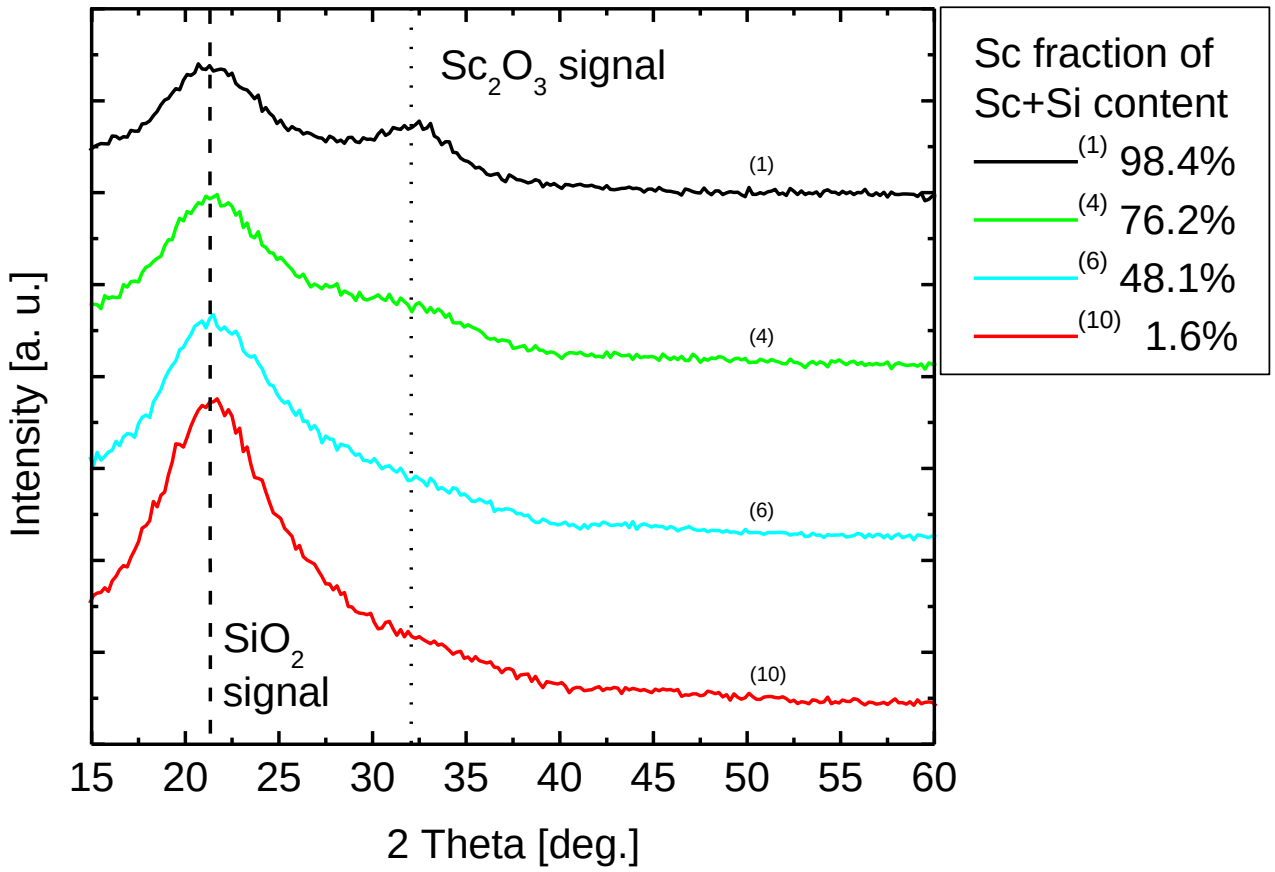
Sc fraction of
Sc+Si content
(1) 98.4%
(4) 76.2%
(6) 48.1%
(10) 1.6%
Sc2O3 signal
SiO2
signal
(1)
(4)
(6)
(10)
Intensity [a. u.]
15 20 25 30 35 40 45 50 55 60
2 Theta [deg.]

Fig. 6

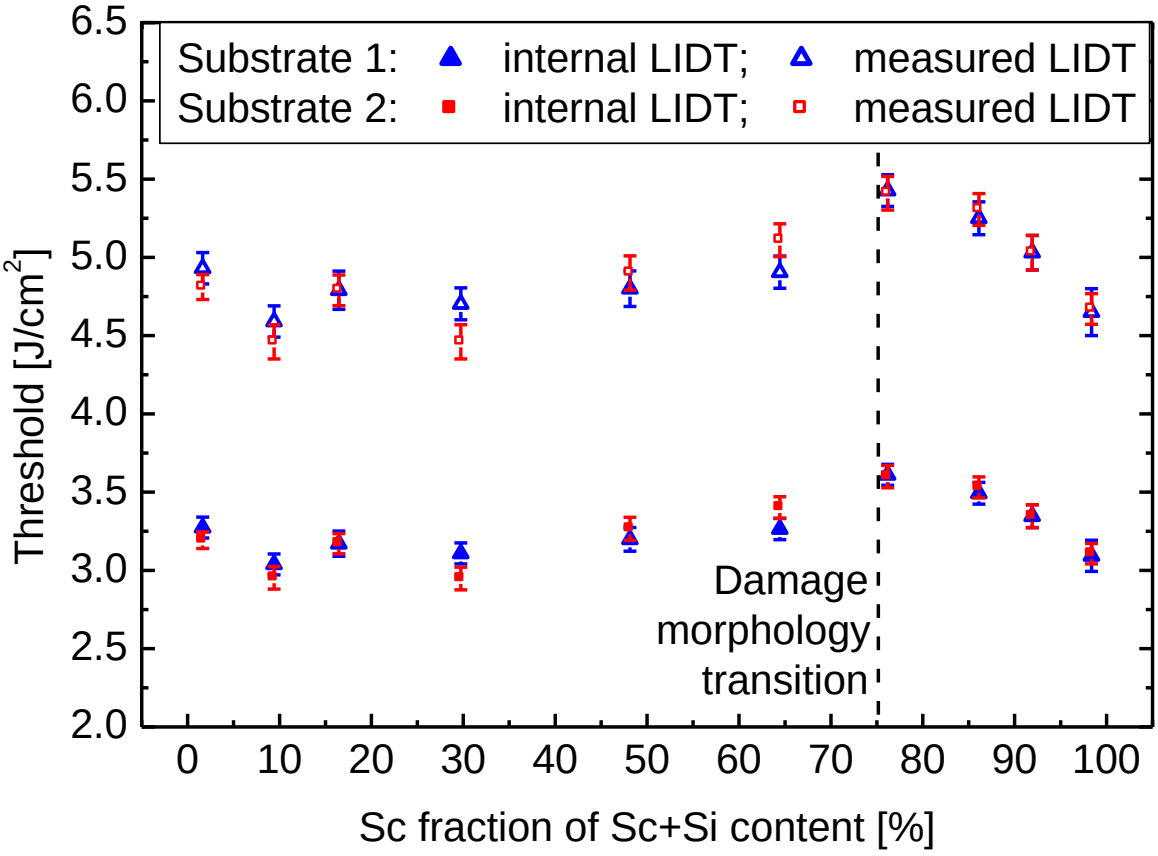
Substrate 1: internal LIDT; measured LIDT
Substrate 2: internal LIDT; measured LIDT
Damage morphology transition
Threshold [J/cm^2]
Sc fraction of Sc+Si content [%]
6.5
6.0
5.5
5.0
4.5
4.0
3.5
3.0
2.5
2.0
0
10
20
30
40
50
60
70
80
90
100

Fig. 7a

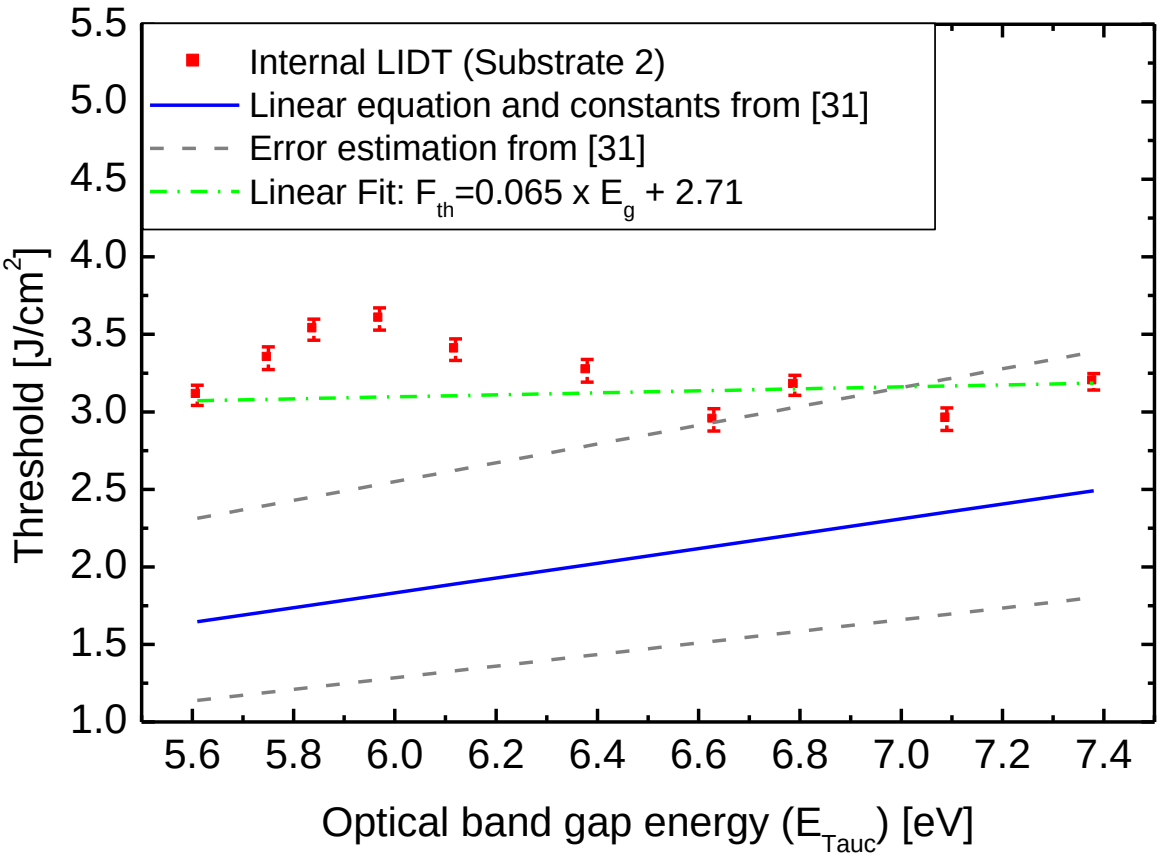
Internal LIDT (Substrate 2)
Linear equation and constants from [31]
Error estimation from [31]
Linear Fit: F_th=0.065 x E_g + 2.71
Threshold [J/cm²]
Optical band gap energy (E_Tauc) [eV]
5.5
5.0
4.5
4.0
3.5
3.0
2.5
2.0
1.5
1.0
5.6
5.8
6.0
6.2
6.4
6.6
6.8
7.0
7.2
7.4

Fig. 7b

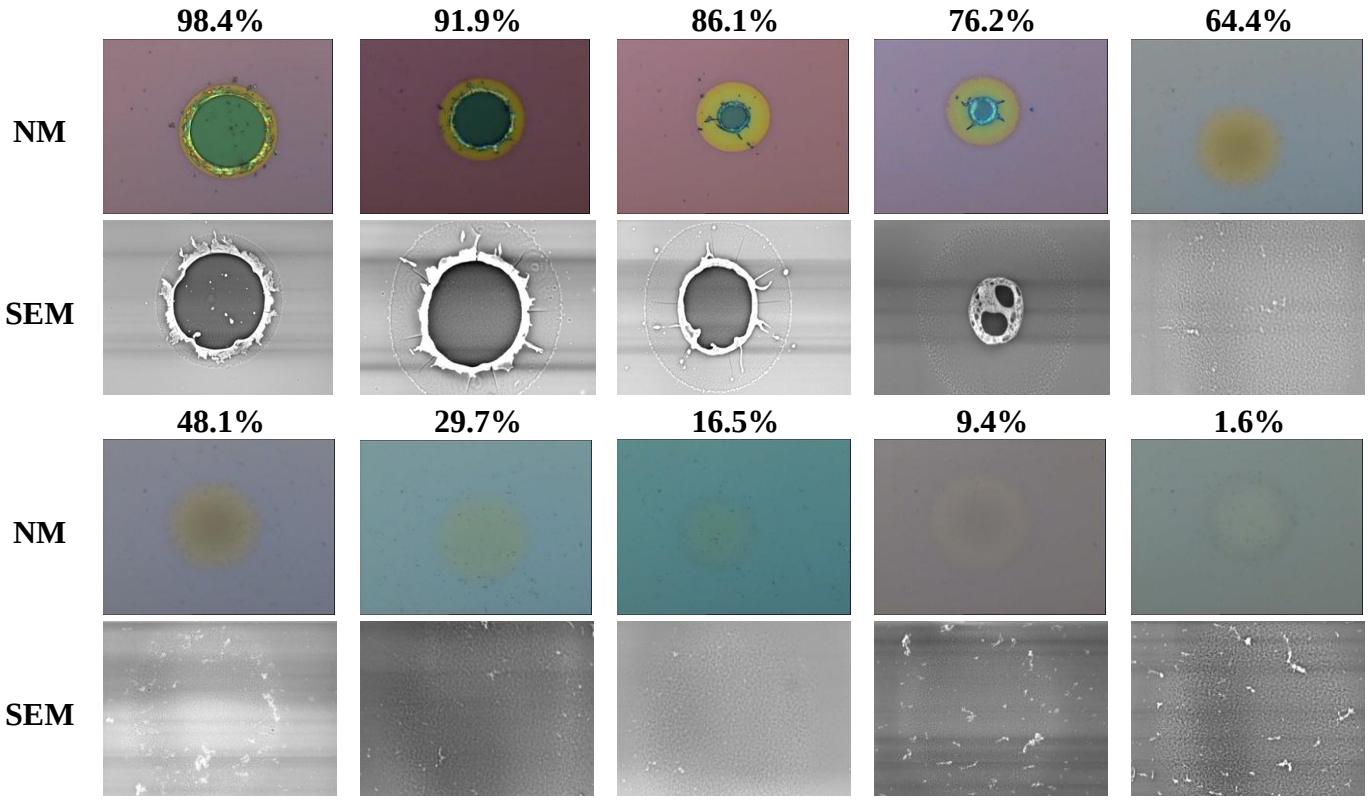

Fig. 8

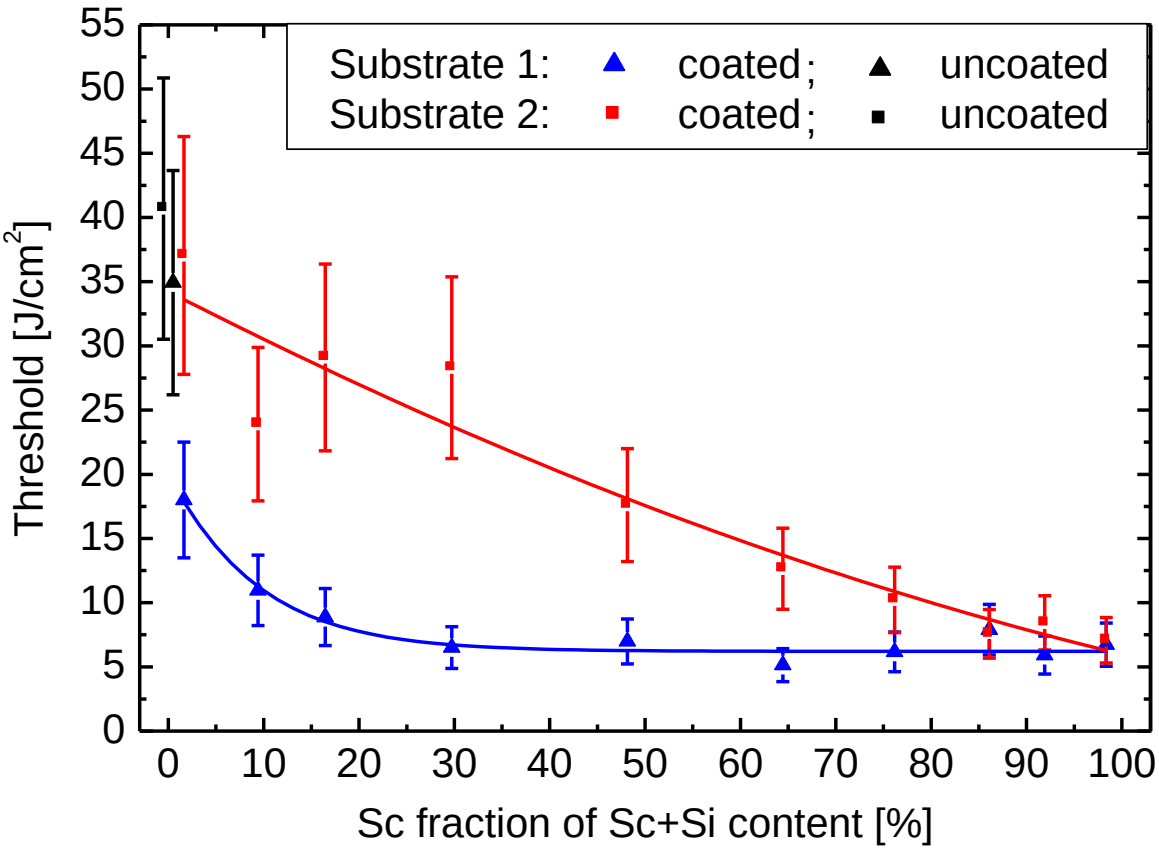
Substrate 1: coated; uncoated
Substrate 2: coated; uncoated
Threshold [J/cm²]
Sc fraction of Sc+Si content [%]
0
5
10
15
20
25
30
35
40
45
50
55
0
10
20
30
40
50
60
70
80
90
100

Fig. 9

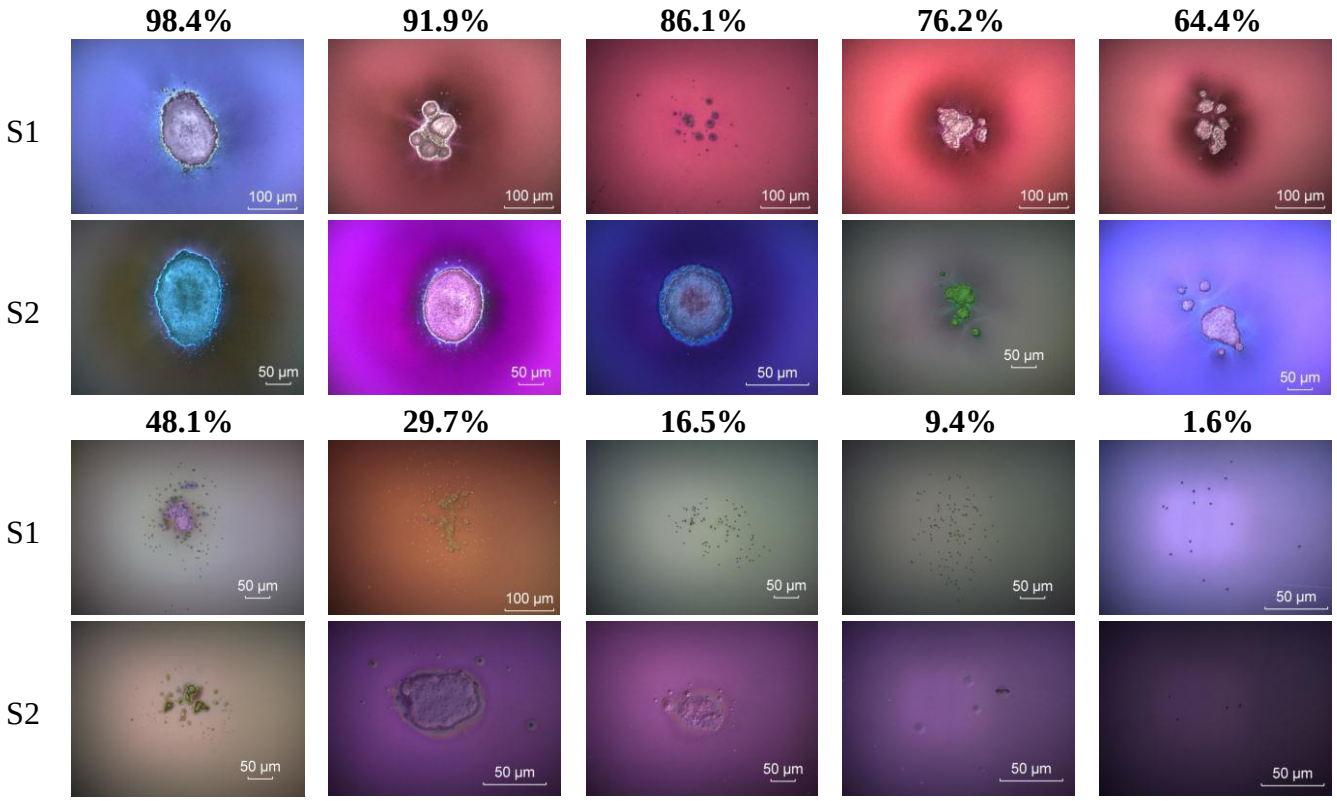

Fig. 10

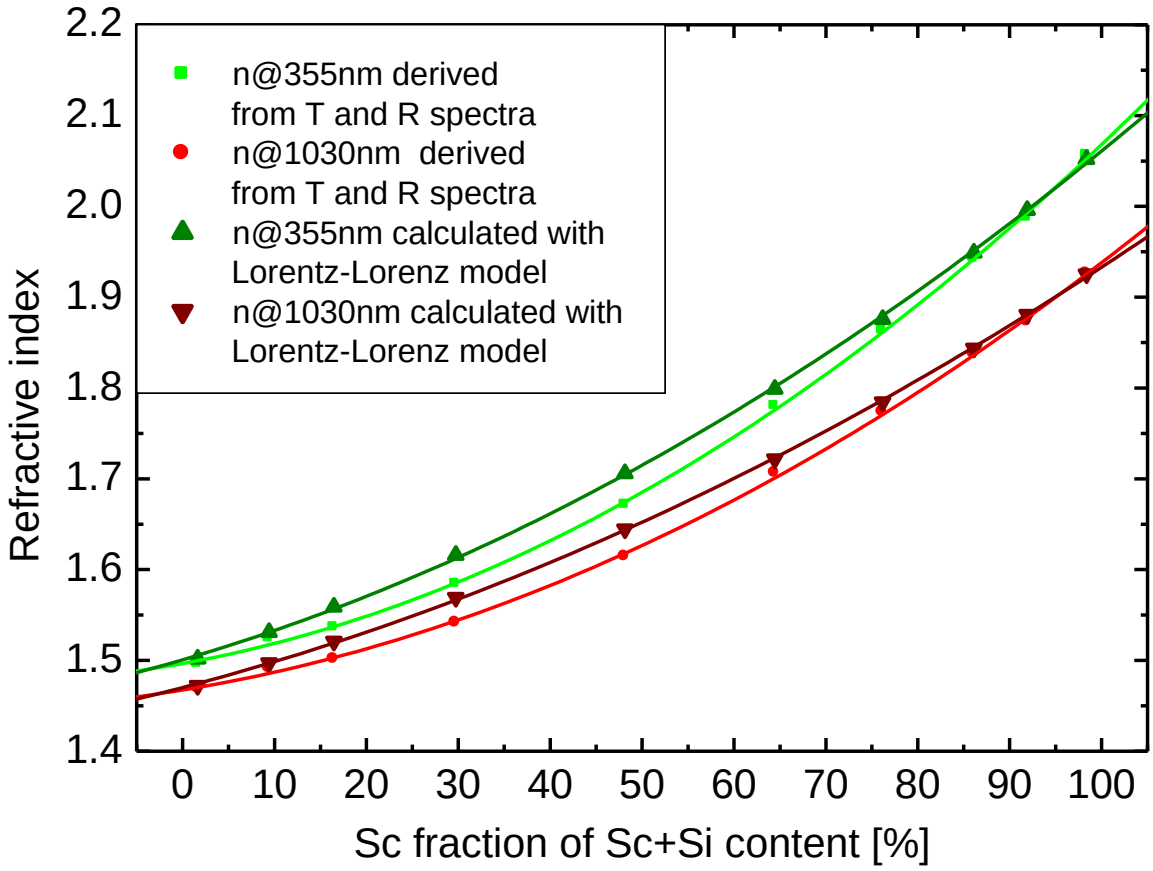
n@355nm derived from T and R spectra
n@1030nm derived from T and R spectra
n@355nm calculated with Lorentz-Lorenz model
n@1030nm calculated with Lorentz-Lorenz model
Refractive index
Sc fraction of Sc+Si content [%]
2.2
2.1
2.0
1.9
1.8
1.7
1.6
1.5
1.4
0
10
20
30
40
50
60
70
80
90
100

Fig. 11

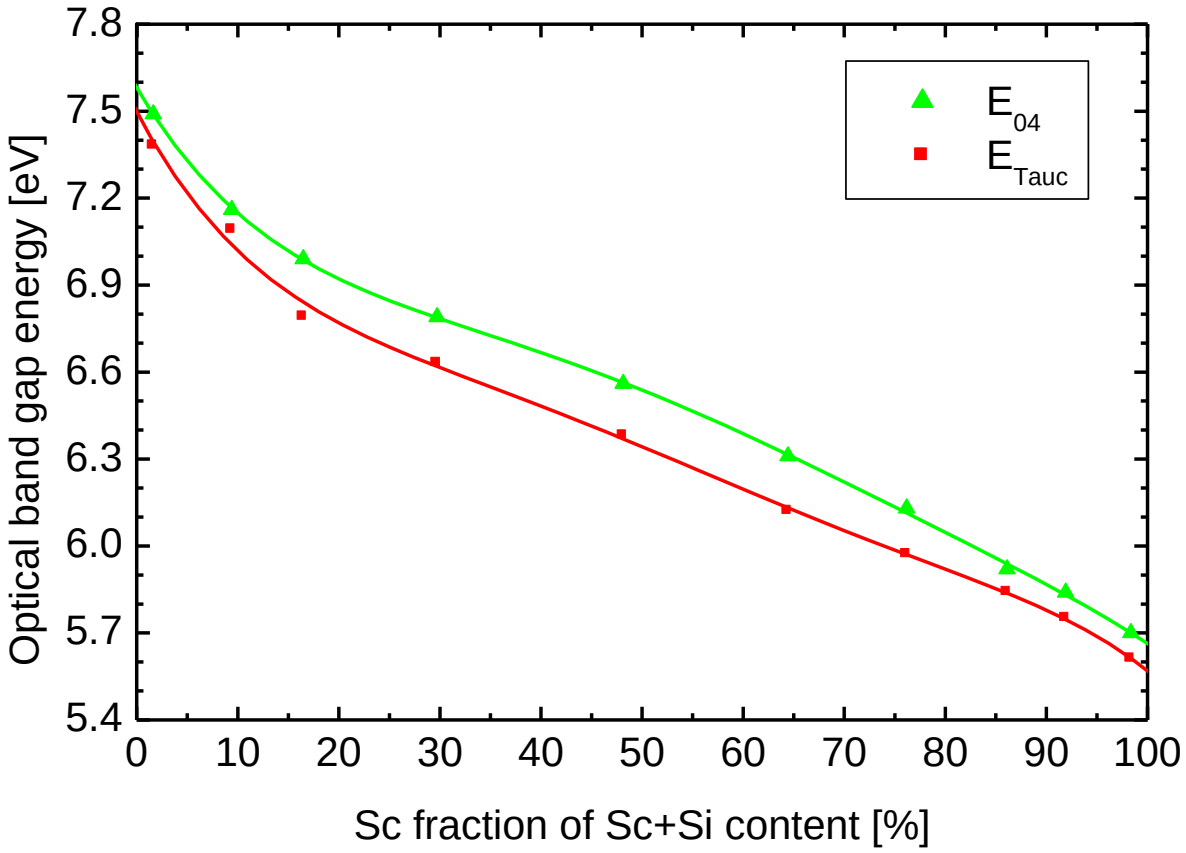
Optical band gap energy [eV]
7.8
7.5
7.2
6.9
6.6
6.3
6.0
5.7
5.4
0
10
20
30
40
50
60
70
80
90
100
Sc fraction of Sc+Si content [%]
E04
ETauc

Fig. 12

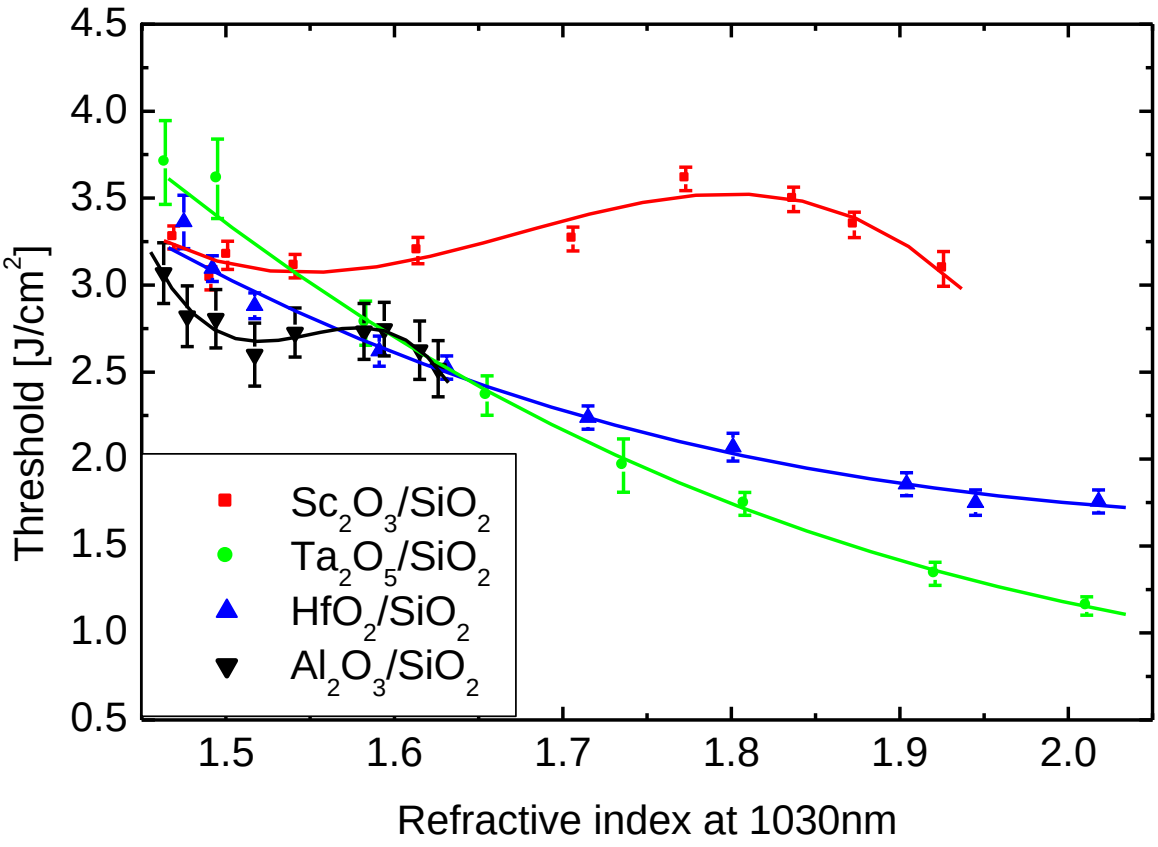
Threshold [J/cm^2]
Refractive index at 1030nm
4.5
4.0
3.5
3.0
2.5
2.0
1.5
1.0
0.5
1.5
1.6
1.7
1.8
1.9
2.0
Sc_2O_3/SiO_2
Ta_2O_5/SiO_2
HfO_2/SiO_2
Al_2O_3/SiO_2

Fig. 13